PLOS | ONE

Scaling Up Stomatal Conductance from Leaf to Canopy Using a Dual-Leaf Model for Estimating Crop Evapotranspiration

Risheng Ding[1], Shaozhong Kang[1]*, Taisheng Du[1], Xinmei Hao[1], Yanqun Zhang[2]

1 Center for Agricultural Water Research in China, China Agricultural University, Beijing, China, 2 National Center of Efficient Irrigation Engineering and Technology Research-Beijing, China Institute of Water Resources and Hydropower Research, Beijing, China

Abstract

The dual-source Shuttleworth-Wallace model has been widely used to estimate and partition crop evapotranspiration (λET). Canopy stomatal conductance (G_{sc}), an essential parameter of the model, is often calculated by scaling up leaf stomatal conductance, considering the canopy as one single leaf in a so-called "big-leaf" model. However, G_{sc} can be overestimated or underestimated depending on leaf area index level in the big-leaf model, due to a non-linear stomatal response to light. A dual-leaf model, scaling up G_{sc} from leaf to canopy, was developed in this study. The non-linear stomata-light relationship was incorporated by dividing the canopy into sunlit and shaded fractions and calculating each fraction separately according to absorbed irradiances. The model includes: (1) the absorbed irradiance, determined by separately integrating the sunlit and shaded leaves with consideration of both beam and diffuse radiation; (2) leaf area for the sunlit and shaded fractions; and (3) a leaf conductance model that accounts for the response of stomata to PAR, vapor pressure deficit and available soil water. In contrast to the significant errors of G_{sc} in the big-leaf model, the predicted G_{sc} using the dual-leaf model had a high degree of data-model agreement; the slope of the linear regression between daytime predictions and measurements was 1.01 ($R^2 = 0.98$), with RMSE of 0.6120 mm s^{-1} for four clear-sky days in different growth stages. The estimates of half-hourly λET using the dual-source dual-leaf model (DSDL) agreed well with measurements and the error was within 5% during two growing seasons of maize with differing hydrometeorological and management strategies. Moreover, the estimates of soil evaporation using the DSDL model closely matched actual measurements. Our results indicate that the DSDL model can produce more accurate estimation of G_{sc} and λET, compared to the big-leaf model, and thus is an effective alternative approach for estimating and partitioning λET.

Citation: Ding R, Kang S, Du T, Hao X, Zhang Y (2014) Scaling Up Stomatal Conductance from Leaf to Canopy Using a Dual-Leaf Model for Estimating Crop Evapotranspiration. PLoS ONE 9(4): e95584. doi:10.1371/journal.pone.0095584

Editor: Ben Bond-Lamberty, DOE Pacific Northwest National Laboratory, United States of America

Received November 10, 2013; **Accepted** March 28, 2014; **Published** April 21, 2014

Funding: This research was partially supported by the National Natural Science Foundation of China (51321001 and 51309223), the National High-Tech Research and Development Program (2011AA100502 and 2013AA102904) and the Ph.D. Programs Foundation of Ministry of Education of China (20130008120007). The research is also supported by the Program of Introducing Talents of Discipline to Universities (B14002). The funders had no role in study design, data collection and analysis, decision to publish, or preparation of the manuscript.

Competing Interests: The authors have declared that no competing interests exist.

* E-mail: kangsz@cau.edu.cn

Introduction

Accurate estimation of evapotranspiration (λET) is important in understanding terrestrial hydrological cycles because λET is the largest component in the terrestrial water balance after precipitation [1]. In agricultural production, improved estimation of crop λET is also needed to develop precise irrigation scheduling and enhance water use efficiency, as soil water depletion is mostly determined by the rate of λET [2,3,4]. However, direct measurement of λET is often difficult, costly and not available in many regions [5,6]. Therefore, mathematical models are needed to estimate λET using readily measurable meteorological and environmental variables.

Vegetation transpiration (T_r) and soil evaporation (E_s), which are controlled by different biotic and physical processes, are the two major components of λET. Transpiration is strongly linked to crop productivity since it occurs concurrently with photosynthetic gas exchange [7]. Quantifying T_r is also critical to accurately predict the response of crop functioning and physiology to changing climate [8]. Because the two separate processes occur simultaneously, there is no simple way to distinguish between them [9,10].

Several models have been developed to calculate λET and separately estimate soil evaporation and transpiration [11,12,13]. Shuttleworth and Wallace [14] described a dual-source model with a resistance-energy combination, which could separately predict T_r and E_s, and is also sufficiently simple [8]. This model has been widely used and can also be used to gain an understanding of the interaction of biophysical and hydrological processes in the crop canopy [14,15]. Determination of different resistances or conductances (the reciprocal of resistance) is necessary for its practical application. Specifically, canopy stomatal conductance (G_{sc}) is often calculated by scaling up leaf stomatal conductance of the leaves acting in parallel while treating the canopy as one big-leaf, hereafter the big-leaf approach [8,16].

The weakness of using the big-leaf approach is that the use of mean absorbed radiation can significantly overestimate G_{sc}, especially in dense canopies, because the light response of stomata

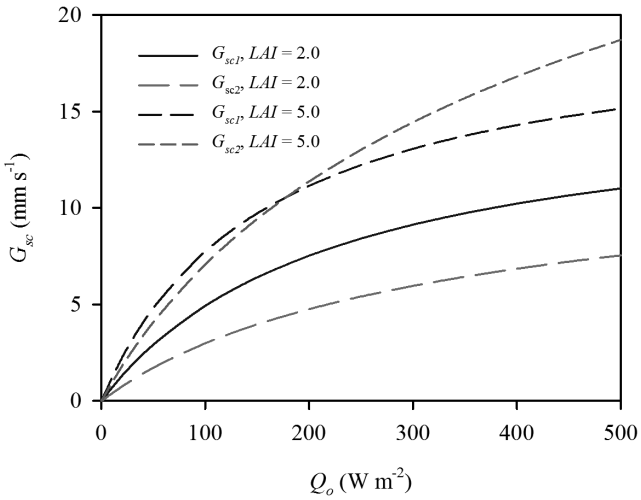

Figure 1. Response of canopy stomatal conductance (G_{sc}) to incident PAR above the canopy (Q_o) at different leaf area indices (*LAI*). G_{sc1} and G_{sc2} are calculated by the big-leaf and dual-leaf canopy stomatal resistance models, respectively.
doi:10.1371/journal.pone.0095584.g001

is non-linear [17,18]. Moreover, the overestimation of G_{sc} by the big-leaf approach often occurred when using total leaf area index (*LAI*) to scale up stomatal conductance. To mitigate the overestimation of G_{sc}, researchers have used the effective or sunlit *LAI* (LAI_e) instead of total *LAI* [16,18]. But, the relationship between LAI_e and *LAI* is empirical and varies with the vegetation type and solar radiation angle. Therefore, models of G_{sc} should consider the non-linear response of stomata to irradiance as well as heterogeneous radiation profiles in the canopy. Beam and diffuse radiation penetrating the canopy must be considered separately due to differential attenuation in canopies, as should visible and near-infrared wavebands due to differential absorption by leaves [12,19]. A multilayers model could account for the mechanism of radiation penetration [20,21], but it is useless in practical applications [22]. Some studies indicate that radiation penetration within the canopy could be simplified by splitting the canopy into two fractions of leaves: sunlit and shaded [18,23,24]. Leuning et al. [25] used a multilayer model to show that photosynthesis from a canopy is closely approximated when calculated as the separate sums of sunlit and shaded fractions, weighted by their respective leaf area within the canopy. However, few studies have calculated G_{sc} using the approach of sunlit and shaded leaves (hereafter, the dual-leaf approach) in the dual-source S-W model for estimating λET.

Soil surface resistance (r_{ss}) is another key parameter for partitioning λET in the dual-source model because above-canopy λET is contaminated by flux from the soil substrate as variations in leaf area affect soil exposure, soil evaporation and absorbed radiation [14,26]. To reduce soil evaporation in the field, the ground is often mulched with plastic film, and this technique is widely used in northwest China [10,27]. But the effect of ground mulching on soil evaporation has not been taken into account when parameterizing r_{ss} in the dual-source model. In this study, a dual-leaf model of G_{sc} was developed by scaling up leaf stomatal conductance using the corresponding absorbed irradiance for the sunlit and shaded leaves separately, which overcomes the limitations of the big-leaf model. The dual-leaf model developed here was then incorporated into the dual-source model to estimate and partition λET. We evaluated the dual-source dual-leaf model (DSDL) by comparing the model estimations of λET with measurements taken in an irrigated maize field mulched with plastic film.

Model Development for Evapotranspiration and Canopy Stomatal Conductance

1 Dual-source Evapotranspiration Model

The λET in the dual-source model was partitioned into two components, canopy transpiration (λT_c) and soil evaporation (λE_s) with a resistance network [14].

$$\lambda ET = \lambda T_c + \lambda E_s = \omega_c PM_c + \omega_s PM_s \tag{1}$$

$$PM_c = \frac{\Delta A + \left(\rho C_p VPD - \Delta r_{ac} A_s\right)/(r_{aa} + r_{ac})}{\Delta + \gamma[1 + r_{sc}/(r_{aa} + r_{ac})]} \tag{2}$$

$$PM_s = \frac{\Delta A + \left[\rho C_p VPD - \Delta r_{as}(A - A_s)\right]/(r_{aa} + r_{as})}{\Delta + \gamma[1 + r_{ss}/(r_{aa} + r_{as})]} \tag{3}$$

$$\omega_c = \frac{1}{1 + R_c R_a/[R_s(R_c + R_a)]} \tag{4}$$

$$\omega_s = \frac{1}{1 + R_s R_a/[R_c(R_s + R_a)]} \tag{5}$$

$$R_s = (\Delta + \gamma) r_{as} + \gamma r_{ss} \tag{6}$$

$$R_c = (\Delta + \gamma) r_{ac} + \gamma r_{sc} \tag{7}$$

$$R_a = (\Delta + \gamma) r_{aa} \tag{8}$$

where PM_c and PM_s are the terms similar to those in Penman–Monteith model for canopy transpiration and soil evaporation, respectively, and ω_c and ω_s are the weighting factors for the crop canopy and soil components, respectively. λ is the heat of water vaporization, ρ is air density, C_p is the specific heat of dry air at constant pressure, Δ is the slope of the saturation vapor pressure curve, γ is the psychrometric constant, *VPD* is vapor pressure deficit, and A and A_s are the total available energy and available energy for soil, respectively. r_{sc} is canopy stomatal resistance, r_{ss} is soil surface resistance, r_{ac} is canopy boundary layer resistance, r_{as} is soil boundary layer resistance between soil and vegetative canopy, and r_{aa} is aerodynamic resistance between canopy source and reference height, respectively. The calculation procedures of the other resistances except r_{sc} and r_{ss} are given in Appendix S1.

$$A = R_n - G \tag{9}$$

$$A_s = R_{ns} - G \tag{10}$$

$$R_{ns} = R_n \exp(-\kappa_R LAI) \tag{11}$$

where R_n and R_{ns} are net radiation above the canopy and at the soil surface, respectively, and G is the soil heat flux. The canopy extinction coefficient of net radiation, κ_R, is dependent on leaf orientation and solar zenith angle (ζ) [17].

$$\kappa_R = \frac{G_L}{\cos(\zeta)} \tag{12}$$

where G_L is 0.5 for a spherical leaf angle distribution. ζ, the angle subtended by the sun at the center of the earth, is perpendicular to the surface of the earth and calculated as in Appendix S1.

The two components, λT_c and λE_s were now calculated along with the *VPD* at the canopy source height (D_o).

$$D_o = VPD + [\Delta A - (\Delta + \gamma)\lambda ET] r_{aa} / \rho C_p \tag{13}$$

$$\lambda T_c = \frac{\Delta(A - A_s) + \rho C_p D_o / r_{ac}}{\Delta + \gamma(1 + r_{sc}/r_{ac})} \tag{14}$$

$$\lambda E_s = \frac{\Delta A_s + \rho C_p D_o / r_{as}}{\Delta + \gamma(1 + r_{ss}/r_{as})} \tag{15}$$

The measured r_{sc} was obtained by inverting Eq. (14), with λT_c calculated by the known or measured λET and λE_s.

$$\lambda T_c = \lambda ET - \lambda E_s \tag{16}$$

$$r_{sc} = \frac{\Delta(A - A_s) + \rho_a C_p D_o / r_{ac} - \lambda T_c(\Delta + \gamma)}{\gamma \lambda T_c / r_{ac}} \tag{17}$$

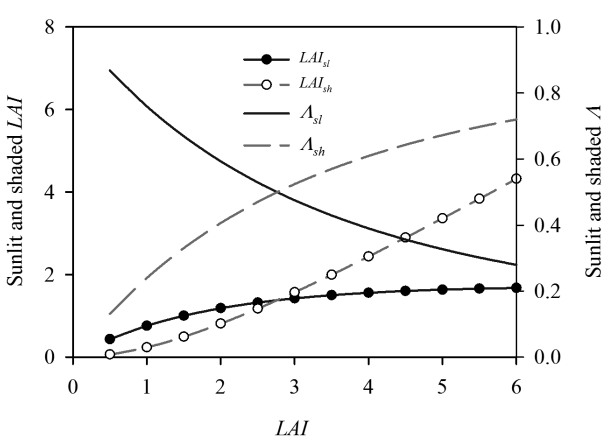

Figure 2. Variation in the sunlit and shaded leaf area indices (LAI_{sl} and LAI_{sh}) versus different *LAI*. The ratios of LAI_{sl} and LAI_{sh} to *LAI* (Λ_{sl} and Λ_{sh}) are also shown.
doi:10.1371/journal.pone.0095584.g002

2 Irradiance within Crop Canopy

Incident PAR light above the canopy (Q_o) was divided into diffuse (Q_{od}) and beam irradiance (Q_{ob}) through the fraction of diffuse radiation (f_d).

$$Q_{od} = f_d Q_o \tag{18}$$

$$Q_{ob} = (1 - f_d) Q_o \tag{19}$$

The f_d was calculated from a simple model of atmospheric attenuation of radiation [17,28].

$$f_d = \frac{1 - \tau_a{}^{m_a}}{1 + \tau_a{}^{m_a}(1/f_a - 1)} \tag{20}$$

where τ_a is the atmospheric transmittance, f_a is the forward scattering coefficient of PAR in atmosphere, and m_a is the optical air mass, which can be calculated as follows.

$$m_a = \frac{P/P_o}{\cos\zeta} \tag{21}$$

where P is local atmospheric pressure and P_0 is atmospheric pressure at sea level.

At a depth ξ in the canopy, three types of irradiance can be calculated: the total beam, $Q_{\ell,bt}$ (unintercepted beam plus down scattered beam), direct beam, $Q_{\ell,b}$ (unintercepted beam) and the diffuse flux, $Q_{\ell,d}$ [17,29].

$$Q_{\ell,bt}(\xi) = Q_{ob}(1 - \rho_{cb})\sqrt{\alpha}\kappa_b \exp\left(-\sqrt{\alpha}\kappa_b \xi\right) \tag{22}$$

$$Q_{\ell,b}(\xi) = Q_{ob}(1 - \rho_{cb})\kappa_b \exp(-\kappa_b \xi) \tag{23}$$

$$Q_{\ell,d}(\xi) = Q_{od}(1 - \rho_{cd})\sqrt{\alpha}\kappa_d \exp\left(-\sqrt{\alpha}\kappa_d \xi\right) \tag{24}$$

$$\rho_{cb} = 1 - \exp(2\rho_h \kappa_b / (1 + \kappa_b)) \tag{25}$$

$$\rho_h = \frac{1 - \sqrt{\alpha}}{1 + \sqrt{\alpha}} \tag{26}$$

$$\rho_{cd} = \frac{2\kappa_d \rho_h}{\kappa_d + 1} \tag{27}$$

where α is absorptivity of leaves for irradiation, ρ_{cb} and ρ_{cd} are canopy reflectance for beam and diffuse irradiance respectively with a randomly spherical leaf-angle distribution, ρ_h is canopy reflectance for beam irradiance with a horizontal leaf-angle distribution, and κ_d is an extinction coefficient for diffuse radiation.

The absorbed irradiance in a canopy height (Q_ℓ) consists of the total beam radiation ($Q_{\ell,bt}$) and the diffuse radiation ($Q_{\ell,d}$).

$$Q_\ell(\xi) = Q_{\ell,bt}(\xi) + Q_{\ell,d}(\xi) \tag{28}$$

The total irradiance absorbed by the entire canopy (Q_c) per unit ground area was determined by integrating Q_ℓ over the total *LAI*.

$$Q_c = \int_0^{LAI} Q_l(\xi)d\xi = Q_{ob}(1-\rho_{cb})\left[1-\exp\left(-\sqrt{\alpha}\kappa_b LAI\right)\right] + Q_{od}(1-\rho_{cd})\left[1-\exp\left(-\sqrt{\alpha}\kappa_d LAI\right)\right] \quad (29)$$

The irradiance absorbed by the sunlit fraction in a specific canopy height ($Q_{\ell,sl}$) can be given as the sum of direct-beam ($Q_{\ell,b}$), diffuse ($Q_{\ell,d}$) and scattered-beam components ($Q_{\ell,s}$).

$$Q_{\ell,sl}(\xi) = Q_{\ell,b}(\xi) + Q_{\ell,d}(\xi) + Q_{\ell,s}(\xi) \quad (30)$$

$$Q_{\ell,s}(\xi) = Q_{0b}\left[(1-\rho_{cb})\sqrt{\alpha}\kappa_b \exp\left(-\sqrt{\alpha}\kappa_b\xi\right) - \alpha\kappa_b \exp(-\kappa_b\xi)\right] \quad (31)$$

The irradiance absorbed by the sunlit fraction in the entire canopy (Q_{sl}) was obtained by integrating $Q_{\ell,sl}$ over the total *LAI*.

$$Q_{sl} = \int_0^{LAI} Q_{\ell,sl}(\xi)f_{\ell,sl}(\xi)d\xi = \int_0^{LAI} Q_{\ell,b}(\xi)f_{\ell,sl}(\xi)d\xi + \int_0^{LAI} Q_{\ell,d}(\xi)f_{\ell,sl}(\xi)d\xi + \int_0^{LAI} Q_{\ell,s}(\xi)f_{\ell,sl}(\xi)d\xi \quad (32)$$

$$\int_0^{LAI} Q_{\ell,b}(\xi)f_{\ell,sl}(\xi)d\xi = Q_{ob}\alpha[1-\exp(-\kappa_b LAI)] \quad (32a)$$

$$\int_0^{LAI} Q_{\ell,d}(\xi)f_{\ell,sl}(\xi)d\xi = Q_{od}(1-\rho_{cd})\frac{\sqrt{\alpha}\kappa_d}{\sqrt{\alpha}\kappa_d+\kappa_b}\left[1-\exp\left(-\left(\sqrt{\alpha}\kappa_d+\kappa_b\right)LAI\right)\right] \quad (32b)$$

$$\int_0^{LAI} Q_{\ell,s}(\xi)f_{\ell,sl}(\xi)d\xi = Q_{ob}\left[(1-\rho_{cb})\frac{\sqrt{\alpha}}{\sqrt{\alpha}+1}\left(1-\exp\left(-\left(\sqrt{\alpha}\kappa_b+\kappa_b\right)LAI\right)\right) - \alpha(1-\exp(-2\kappa_b LAI))/2\right] \quad (32c)$$

The total irradiance absorbed (Q_c) is the sum of the two parts, irradiance absorbed by the separate sunlit (Q_{sl}) and shade fractions (Q_{sh}) of the canopy. Thus, Q_{sh} was calculated as the difference between Q_c and Q_{sl}.

$$Q_{sh} = Q_c - Q_{sl} \quad (33)$$

3 Leaf and Canopy Stomatal Conductance

The stomatal conductance is represented by g_s for a single leaf and G_{sc} for the entire canopy.

3.1. Leaf stomatal conductance. The leaf g_s can be calculated using the Jarvis-Stewart type multiple formulae [30,31,32].

$$g_s = \frac{1}{r_s} = g_{smax}\,\Pi_i\,F_{X_i} \quad (34)$$

where g_{smax} is the maximum value of the leaf stomatal conductance and Fx_i is the stress function of the specific environmental variables (x_i), $0 \le Fx_i \le 1$. The original model used short-wave radiation as the light variable. Here we have used the photosynthetically active radiation absorbed by canopy leaves (Q_a) because stomatal aperture is determined by the received visible wavelength radiation, rather than short-wave radiation [17,18,33]. In addition, we incorporated the environmental stress impact on g_s by *VPD* and available soil water as follows.

$$F_Q = \frac{500+k_Q}{500}\frac{Q_a}{Q_a+k_Q} \quad (35)$$

$$F_D = e^{-k_D VPD} \quad (36)$$

$$F_w = \frac{1-\exp(-k_w\theta_E)}{1-\exp(-k_w)} \quad (37)$$

$$\theta_E = \frac{\theta-\theta_W}{\theta_F-\theta_W} \quad (38)$$

where the k_Q, k_D and k_w are the stress coefficients of Q_a, *VPD* and extractable soil water in the root zone (θ_E), and θ, θ_F and θ_W are the measured soil moisture, field capacity and wilting point in the root zone, respectively.

3.2. Big-leaf model of canopy stomatal conductance. The canopy stomatal conductance in the big-leaf model (G_{sc1}) is estimated by scaling up g_s weighing by the effective *LAI* (LAI_e) as if the canopy is a single big-leaf [16,18,32].

$$G_{sc1} = \frac{1}{r_{sc1}} = g_{s1}LAI_e \quad (39)$$

where g_{s1} is the mean leaf stomatal conductance for the entire big-leaf and can be calculated by Eq. (34) based on the mean absorbed irradiance of the entire canopy using Eq. (29); LAI_e is empirically equal to the actual *LAI* for $LAI \le 2$, $LAI/2$ for $LAI \ge 4$, and 2.0 for others [16].

Table 1. The parameters used in the dual-source dual-leaf model.

Symbol	Description	Value	Units	Sources
b_1	Parameter in soil resistance model	15.2	s m^{-1}	Fitted in this study
b_2	Parameter in soil resistance model	−5.8	-	Fitted in this study
b_3	Parameter in soil resistance model	88.7	s m^{-1}	Fitted in this study
c_d	Mean drag coefficient for the individual vegetative elements	0.1	-	Meyers and Paw [42]
d_l	Characteristic leaf dimension	0.068	m	Measured in this study
G_L	Spherical leaf angle distribution	0.5	-	Campbell and Norman [17]
g_{smax}	Maximum value of the leaf stomatal conductance	7.5	mm s^{-1}	Fitted in this study
k	von Karman's constant	0.41	-	Brutsaert [41]
k_Q	Stress coefficients of the photosynthetically active radiation in the stomatal conductance model	150	W m^{-2}	Fitted in this study
k_D	Stress coefficients of the vapor pressure deficit in the stomatal conductance model	0.2	kPa^{-1}	Fitted in this study
k_w	Stress coefficients of the extractable soil water in the root zone in the stomatal conductance model	7.5	-	Fitted in this study
z_{0s}	Effective roughness length of the soil substrate	0.01	m	Shuttleworth and Wallace [14]
α	Absorptivity of leaves of irradiation	0.8	-	Monteith and Unsworth [12]
κ_d	Extinction coefficient for diffuse radiation	0.7	-	Campbell and Norman [17]
τ_a	Atmospheric transmittance	0.72	-	Brutsaert [41]
f_a	Forward scattering coefficient of PAR in the atmosphere	0.43	-	Brutsaert [41]
f_m	Fraction of ground mulched by plastic film	0.5/0.6[a]	-	Measured in this study

[a]0.5/0.6 is the fraction of ground mulched by plastic film in 2009 and 2010, respectively.

doi:10.1371/journal.pone.0095584.t001

3.3. Dual-leaf model of canopy stomatal conductance. In the dual-leaf model, G_{sc} (G_{sc2}) is calculated by summing the contributions of sunlit and shaded fractions, G_{sl} and G_{sh}, respectively, which are scaled up using the associated g_s weighted by their respective fractions of LAI [18,24].

$$G_{sc2}=\frac{1}{r_{sc2}}=G_{sl}+G_{sh}=g_{sl}LAI_{sl}+g_{sh}LAI_{sh} \tag{40}$$

where g_{sl} and g_{sh} are the mean leaf stomatal conductance for sunlit and shaded leaves, respectively, and can be calculated by Eq. (34) based on the separate absorbed irradiance using Eqs. (32) and (33). LAI_{sl} and LAI_{sh} are LAI for sunlit and shaded leaves in the entire canopy, respectively.

Assuming that all leaves in a canopy are randomly distributed, the fraction of sunlit leaves ($f_{\ell,sl}$) in a specific canopy depth declines exponentially with cumulative leaf area (ξ) [29,34].

$$f_{\ell,sl}(\xi)=\exp(-\kappa_b\xi) \tag{41}$$

$$\xi(z)=\int_z^{h_c} L_d(z)dz \tag{42}$$

where κ_b is an extinction coefficient for beam radiation, L_d is leaf area density, z is height above ground, and h_c is canopy height. LAI_{sl} is therefore calculated by integrating $f_{\ell,sl}$ for the entire canopy.

$$LAI_{sl}=\int_0^{LAI} f_{\ell,sl}(\xi)d\xi=\frac{1-\exp(-\kappa_b LAI)}{\kappa_b} \tag{43}$$

$$LAI_{sh}=LAI-LAI_{sl} \tag{44}$$

4 Soil Surface Resistance

In this study, r_{ss} was directly calculated with a function dependent on surface soil water content [35], accounting for the effect of plastic mulching on reduction of soil evaporation by introducing a term for fraction of plastic mulch, f_m [i.e. r_{ss} is divided by the area of exposed substrate per unit ground area ($1-f_m$)].

$$r_{ss}=\frac{1}{1-f_m}\left[b_1\left(\frac{\theta_g}{\theta_s}\right)^{b_2}+b_3\right] \tag{45}$$

where θ_g is the average soil water content between 0–0.1 m, θ_s is the saturated water content of surface soil, and b_1, b_2, and b_3 are the empirical coefficients.

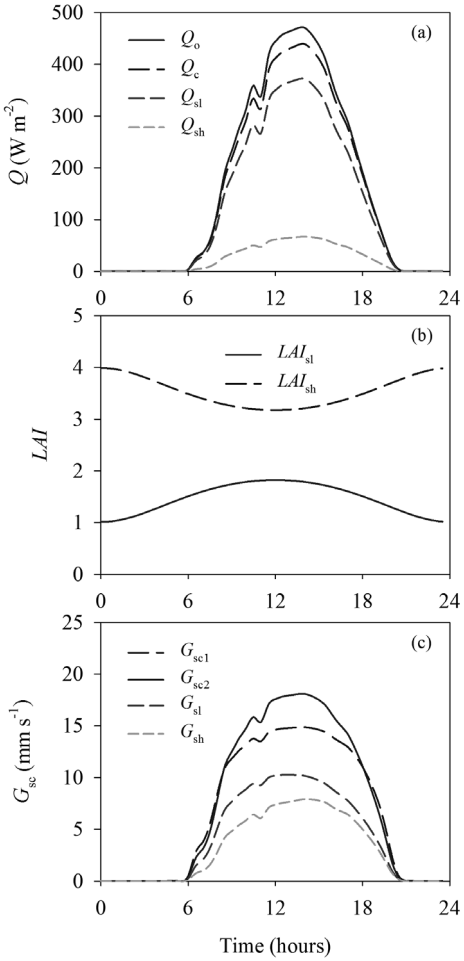

Figure 3. Diurnal variations of (a) modeled irradiance, (b) leaf area index and (c) canopy stomatal conductance at leaf area index (*LAI*) = 5.0. Q_o is the total irradiance above the canopy, Q_c is the irradiance absorbed by the entire canopy, and is separated into the irradiance absorbed by the sunlit leaves of the canopy (Q_{sl}) and irradiance absorbed by the shaded leaves of the canopy (Q_{sh}). LAI_{sl} and LAI_{sh} are the sunlit and shaded fractions of *LAI*, respectively. G_{sc1} and G_{sc2} are the canopy stomatal conductance calculated by the big-leaf and dual-leaf models, respectively; G_{sc2} is separated into the sunlit and shaded canopy stomatal resistance, G_{sl} and G_{sh}, respectively.
doi:10.1371/journal.pone.0095584.g003

Materials and Methods

1 Experimental Arrangement

The experiments were conducted in an irrigated maize field in 2009 and 2010 at Shiyanghe Experimental Station for Water-saving in Agriculture and Ecology of the China Agricultural University in Gansu Province in northwest China (N 37°52′, E 102°50′, Altitude 1581 m). Grain maize was sown on April 21 and May 2, and harvested on September 28 and September 26 in 2009 and 2010, respectively. The ground was partly mulched with plastic films with a width of 100 cm, and there was bare soil of 65 and 45 cm in width between two film rows in 2009 and 2010, respectively. Maize seed was sown in holes of 5.0 cm diameter under the plastic films, with a row spacing of 50 and 45 cm and a plant spacing of 24 and 23 cm for 2 years. Maize was not sown in the bare soil. This planting scheme had an actual density of 76,300 and 82,500 plants ha^{-1} for 2009 and 2010, respectively. Actual fractions of ground-mulching were ~0.5 and 0.6, respectively, which were defined as one minus the ratio of the summed surface areas of bare soil and holes to ground area. For the 0–1.0 m soil depth, the soil type was silt loam, with a bulk density of 1.38 g cm^{-3}, a field capacity of 0.30 m^3 m^{-3}, and a wilting point of 0.12 m^3 m^{-3}. Over the entire growing season, maize was border-irrigated four times, with a total irrigation water amount of 420 mm for both years. The amount of each irrigation event was measured by a water meter. Each irrigation amount was 105 mm on June 15, July 6, July 29 and August 20, 2009, and 105, 120, 90, and 105 mm on June 22, July 27, August 5 and August 29, 2010, respectively.

2 Measurements of Evapotranspiration and Soil Evaporation

λET was measured using an eddy covariance (EC) system installed in the center of the maize field. The EC consists of a fast response 3D sonic anemometer (CSAT3, Campbell Scientific Inc., UT, USA), a Krypton hygrometer (KH20, Campbell Scientific Inc.) and a temperature and humidity sensor (HMP45C, Vaisala Inc., Helsinki, Finland). All sensors were connected to a data logger (CR5000, Campbell Scientific, Inc.). The sonic anemometer and Krypton hygrometer were installed at a height of 1.0 m over the crop canopy. Net radiation (R_n) was measured by a net radiometer (NR-LITE, Kipp & Zonen, Delft, Netherlands), installed at a height of 3.5 m. Two soil heat fluxes (HFP01, Hukseflux, Delft, Netherlands) were installed at a soil depth of 8.0 cm under the plastic film and bare soil. Soil temperature above each soil heat flux plate was measured using thermocouples at depths of 0.0 cm, 2.0 cm and 6.0 cm. Soil water content from 0–10.0 cm was measured using a soil moisture reflectometer (EnviroSMART, Sentek Sensor Technologies, SA, Australia). Ground heat flux (G) was estimated by correcting heat fluxes at 8.0 cm for heat storage above the transducers. The heat storage was determined from changes in soil temperature and moisture above the transducers. Based on the covariance of the 10 Hz air temperature and specific humidity with vertical wind velocity, the latent heat flux in 30 min durations was computed using the eddy covariance methodology with the CarboEurope recommendations [36]. Daytime λET was adjusted by the Bowen-ratio forced closure method, and nighttime λET was adjusted using the filtering interpolation method as proposed by Ding et al. [37].

Soil evaporation (E_s) was measured by the micro-lysimeter. Eight micro-lysimeter cylinders, made from PVC tubes with a diameter of 10 cm and height of 20 cm, were installed in bare soil between two plastic film rows. The cylinders were weighed at 20:00 every day by an electric scale with a precision of 0.1 g. The micro-lysimeters were reinstalled within one day after each irrigation and heavy rain. E_s at the field scale can be calculated by weighting the fraction of ground-mulching (f_m) from the following equation.

$$E_s = (1 - f_m) 10 \frac{\overline{\Delta M_s}}{\rho_w A_e} \tag{46}$$

where $\overline{\Delta M_s}$ is the mean weight change of micro-lysimeter every day, A_e is the cross sectional area of the micro-lysimeters (78.5 cm^2 here), ρ_w is water density (1.0 g cm^{-3}) and 10 is a conversion factor for changing units from cm to mm.

3 Other Measurements

Solar radiation, precipitation, air temperature, relative humidity and wind speed were measured with a standard automatic weather station (Hobo, Onset Computer Corp., USA) at a height of 2.0 m

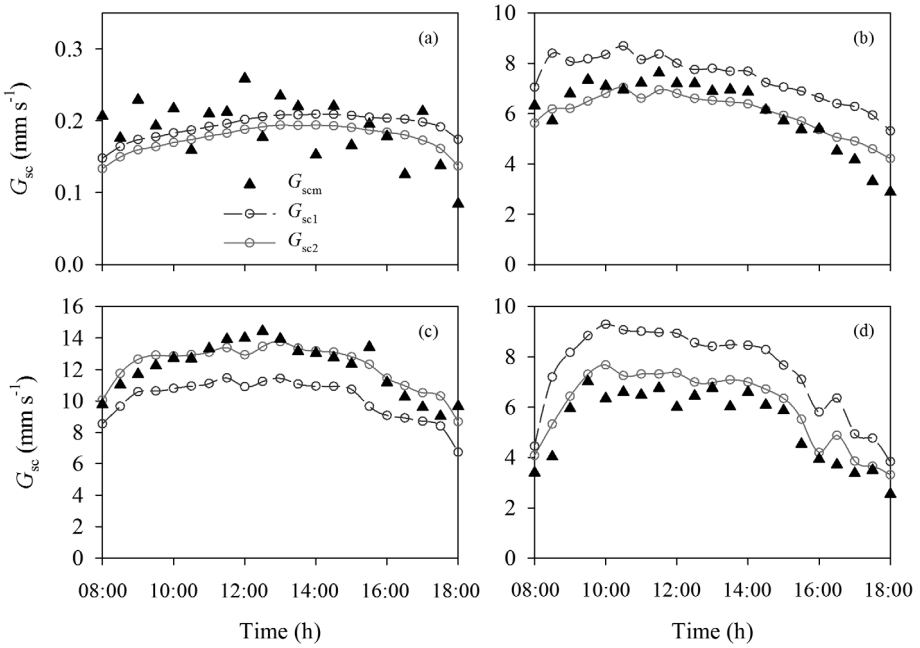

Figure 4. Diurnal variations of half-hourly canopy stomatal conductance (G_{sc}) calculated by the big-leaf (G_{sc1}) and dual-leaf models (G_{sc2}), and measured G_{sc} (G_{scm}) inverted by the S-W model, respectively for four typical clear-sky days in different growth stages of maize in 2009. Leaf area index (*LAI*) was 0.16, 2.62, 5.38 and 2.99, on (a) May 22, (b) June 23, (c) July 27, and (d) September 17, respectively.
doi:10.1371/journal.pone.0095584.g004

above the ground. Volumetric soil water content in the root zone (θ_{rz}) was measured with PVC access tubes using the portable device Diviner 2000 (Sentek Sensor Technologies). Measurements were made at intervals of 0.1 m with a maximal soil depth of 1.0 m at intervals of 3–5 days. Additional samplings were conducted before and after irrigation events, as well as after rainfall events. The measurements were calibrated by oven drying of soil samples. Interpolation was applied between consecutive irrigations to determine θ_r for each day. In addition, two sets of ECH2O probes (Decagon Devices Inc., Pullman, WA, USA) were added to monitor soil moisture at 30 min intervals in 2010.

Ten maize plants were randomly selected to measure leaf length and width, and height at intervals of ~10 days during the growing season. Leaf area was calculated by summing the rectangular area of each leaf (leaf length ×maximum width) multiplied by a factor of 0.74, a conversion factor obtained by analyzing the ratio of the rectangular area to the real area measured by an AM300 (ADC BioScientific Ltd., UK). *LAI* is defined as maize green leaf area per unit ground area. The daily *LAI* was obtained by linear interpolation.

Leaf-scale physiological measurements were performed to derive the stomatal conductance model parameters. A LI-6400 portable photosynthesis system (Li-Cor Inc., Lincoln, NE, USA) was used to measure leaf stomatal conductance on the first fully expanded leaf, which is the fourth leaf counted from the top of the shoot. The diurnal measurements of leaf gas exchange were performed once every 2 h from 8:00 to 18:00 on six sunny days in 10 randomly selected maize plants. Care was taken to keep leaves in their natural positions during measurement. The response of leaf stomatal conductance to varying PAR was measured at 30°C and at a CO_2 concentration of 400 mol mol^{-1} on 29 August, 2009. Measurements were taken at PAR levels of 2000, 1600, 1300, 1000, 800, 600, 400, 200, 100, 50, 20, and 0 μmol m^{-2} s^{-1}. The stomatal light-response curve was fit by a rectangular hyperbola to obtain the parameter values of k_Q using the Jarvis-Stewart model.

4 Model Performance

Half-hourly G_{sc} and λET were calculated using the big-leaf and dual-leaf models Eqs. (39) and (40) with the dual-source equation based on the half-hourly measured meteorological data. The *LAI* and soil water were set as constants at the half-hourly time scale. Daily λET was calculated using Eqs. (39) and (40) with the dual-source equation based on the measured average daily meteorological data. We evaluated the two models by comparing with measurements taken over an irrigated maize field.

The parameters in the Jarvis-Stewart model were obtained using measurements of the stomatal light-response curve and the diurnal leaf gas exchange calculated by non-linear least-squares analysis (SPSS 13.0, SPSS Inc., Chicago, IL, USA). There were ~15 days with no crop cover before the emergence of maize, providing the opportunity to parameterize the empirical coefficients in the soil surface resistance model using the flux observations.

The coefficient of determination (R^2), root mean square error (RMSE) and the Willmott's index of agreement (d) were used to evaluate model performance [38].

Results

1 Model Parameter Estimation and Sensitivity

From the stomatal light-response curve, we obtained best-fitting estimates of k_Q by non-linear least-squares analysis using the Jarvis-Stewart model (Table 1). The stress coefficients of *VPD* and θ_E, k_D and k_w, were optimized using the diurnal measurements of leaf gas exchange (Table 1). Soil surface resistance (r_{ss}) was calculated by inverting the flux-resistance equation for the case of no crops [12]. Based on the relationship between r_{ss} and relative soil water

content (θ_g/θ_s) of the top soil, the best-fitting parameters of b_1, b_2 and b_3 were obtained (Table 1).

The big-leaf model estimates did not closely match the response of G_{sc} to incident PAR above the canopy (Q_c) predicted by the dual-leaf model (Fig. 1). At lower *LAI* (2.0), the big-leaf model overestimated G_{sc} by up to 47.4% at an intermediate irradiance (300 W m^{-2}). At higher *LAI* (5.0), the big-leaf model overestimated G_{sc} when Q_c<200 W m^{-2} and underestimated G_{sc} when Q_c> 200 W m^{-2}. The sensitivity of the dual-leaf model was further analyzed by investigating the variations of the sunlit and shaded leaf area index (LAI_{sl} and LAI_{sh}) against the different *LAI* (Fig. 2). LAI_{sl} approached a maximum of 1.6 when $LAI \geq 3.0$, while LAI_{sh} almost linearly increased as *LAI* increased. As a result, the ratios of LAI_{sl} and LAI_{sh} to *LAI* (Λ_{sl} and Λ_{sh}) nonlinearly decreased and increased, respectively, as *LAI* increased.

The diurnal variations of modeled irradiance absorbed by the entire canopy (Q_c) and its separation into sunlit and shaded fractions (Q_{sl} and Q_{sh}) are shown in Fig. 3a at higher $LAI = 5.0$, using the measured diurnal courses of meteorological and environmental variables from June 23, 2009. Q_c, Q_{sl} and Q_{sh} exhibited the typical diurnal patterns, while Q_{sh} had a lower magnitude than Q_{sl} throughout the day. The average Q_{sl} accounted for 84.2% of the Q_c. The partitioning of leaves into sunlit and shaded fractions continually changes throughout the day (Fig. 3b). LAI_{sl} was a convex parabola, while LAI_{sh} was a concave parabola. The magnitude of LAI_{sh} was greater than LAI_{sl} even during midday when the solar zenith angle is lowest at the higher *LAI*, which is consistent with the result in Fig. 2. The diurnal distributions of G_{sc} calculated by the big-leaf model (G_{sc1}) and dual-leaf model (G_{sc2}) and its separation between sunlit and shaded fractions (G_{sl} and G_{sh}) are presented in Fig. 3c. G_{sc1} was significantly lower than G_{sc2} through most of the day at the higher *LAI*. G_{sh} showed a pattern similar to G_{sl}, while the magnitude of G_{sh} was lower than G_{sl}. The maximum difference between them occurred at the midday around 11:00.

2 Comparisons of Canopy Stomatal Conductance by Big-leaf and Dual-leaf Models

Diurnal patterns of G_{sc} calculated by the big-leaf and dual-leaf models (G_{sc1} and G_{sc2}, respectively) and the measured G_{sc} (G_{scm}) calculated by using Eq. (17) are shown in Fig. 4 for four typical clear-sky days in different growth stages of maize in 2009. The diurnal courses of the G_{sc1} *and* G_{sc2} were similar to the G_{scm}, but there were differences in magnitude. G_{sc1} was significantly lower than G_{scm}, while G_{sc2} closely matched G_{scm} at higher *LAI* (Fig. 4c). G_{sc1} was higher than G_{scm} at the lower *LAI* where there was still good agreement between G_{sc2} and G_{scm} values (Fig. 4b and d). Although the slope of the linear regression between G_{sc1} and G_{scm} was 0.97, G_{sc1} was overestimated at the lower G_{scm} and underestimated at the higher G_{scm} (Fig. 5a), as shown by the lower R^2 of 0.81, greater RMSE of 1.7047 mm s^{-1} and lower d of 0.9563, indicating that the big-leaf model yielded large errors for estimating G_{sc}. In contrast, the slope of the linear regression between G_{sc2} and G_{scm} was 1.01, with an R^2 of 0.98, RMSE of 0.6120 mm s^{-1} and d of 0.9951, indicating that there was good data-model agreement between predictions and measurements (Fig. 5b).

3 Comparisons of Crop Evapotranspiration by Big-leaf and Dual-leaf Models

Diurnal variations of half-hourly λET calculated by the dual-source big-leaf (λET_1) and dual-leaf models (λET_2), and measured λET (λET_m), respectively are presented for four typical clear-sky

Table 2. Comparison of measured and estimated evapotranspiration (λET) and soil evaporation (E_s) during the growth periods of maize in 2009 and 2010.

Years	Time-scales	Models	Average values		Linear regression equation with zero intercept	R^2	RMSE (mm s^{-1})	d
			Measurements (x)	Estimates (y)				
2009	Half-hourly λET	Big-leaf	102.4	79.3	$y = 0.94x$	0.83	72.22	0.9521
		Dual-leaf	102.4	87.6	$y = 1.02x$	0.90	58.06	0.9706
	Daily E_s	Big-leaf	0.44	0.43	$y = 0.95x$	0.63	0.1198	0.9036
		Dual-leaf	0.44	0.46	$y = 1.02x$	0.68	0.1220	0.9129
2010	Half-hourly λET	Big-leaf	107.0	75.2	$y = 0.93x$	0.82	70.97	0.9472
		Dual-leaf	107.0	82.9	$y = 1.03x$	0.88	62.31	0.9626
	Daily E_s	Big-leaf	0.45	0.44	$y = 0.93x$	0.64	0.1593	0.9054
		Dual-leaf	0.45	0.46	$y = 1.01x$	0.73	0.1565	0.9218

Note: R^2 is the coefficient of determination, RMSE is the root mean square error, and d is the Willmott's index of agreement. The units of half-hourly and daily values are W m^{-2} and mm d^{-1}, respectively.

doi:10.1371/journal.pone.0095584.t002

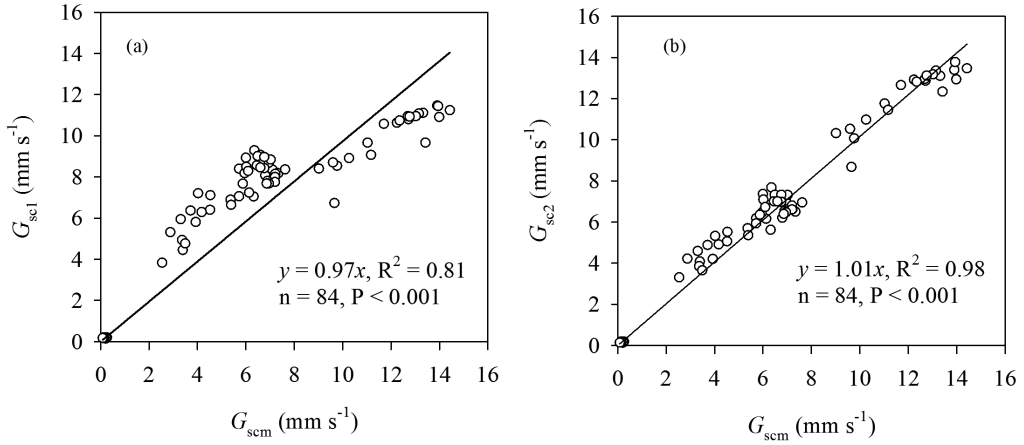

Figure 5. Relationship between canopy stomatal conductance (G_{sc}) estimated by the big-leaf (G_{sc1}) and dual-leaf models (G_{sc2}), and measured G_{sc} (G_{scm}) inverted by the S-W model, respectively for four typical clear-sky days in different growth stages of maize in 2009.
doi:10.1371/journal.pone.0095584.g005

days in different growth stages of maize in 2009 (Fig. 6). The diurnal patterns of estimated λET were similar to the measurements. λET_1 was overestimated at lower *LAI*, and underestimated at higher *LAI*. The linear regression presented that λET_1 was overestimated by 8.7% ($R^2 = 0.97$) and 19.7% ($R^2 = 0.96$) for $LAI = 2.62$ and 2.99, respectively (Fig. 6b and d). λET_1 was underestimated by 13.9% ($R^2 = 0.97$) for $LAI = 5.38$ (Fig. 6c). In contrast, λET_2 had a good agreement with measurements for differing *LAI*, with a linear slope of 1.01 and an R^2 of 0.97.

The irrigation scheduling and mulching fractions in 2009 and 2010 were different (See section 3.1), which yielded different *LAI* and soil water regimes for the two years (See Figure 1 and Table 1 in Ding et al.[39]). The maximum and averaged values of *LAI* respectively were 5.4 and 3.1 for 2009, and 4.7 and 2.7 for 2010.

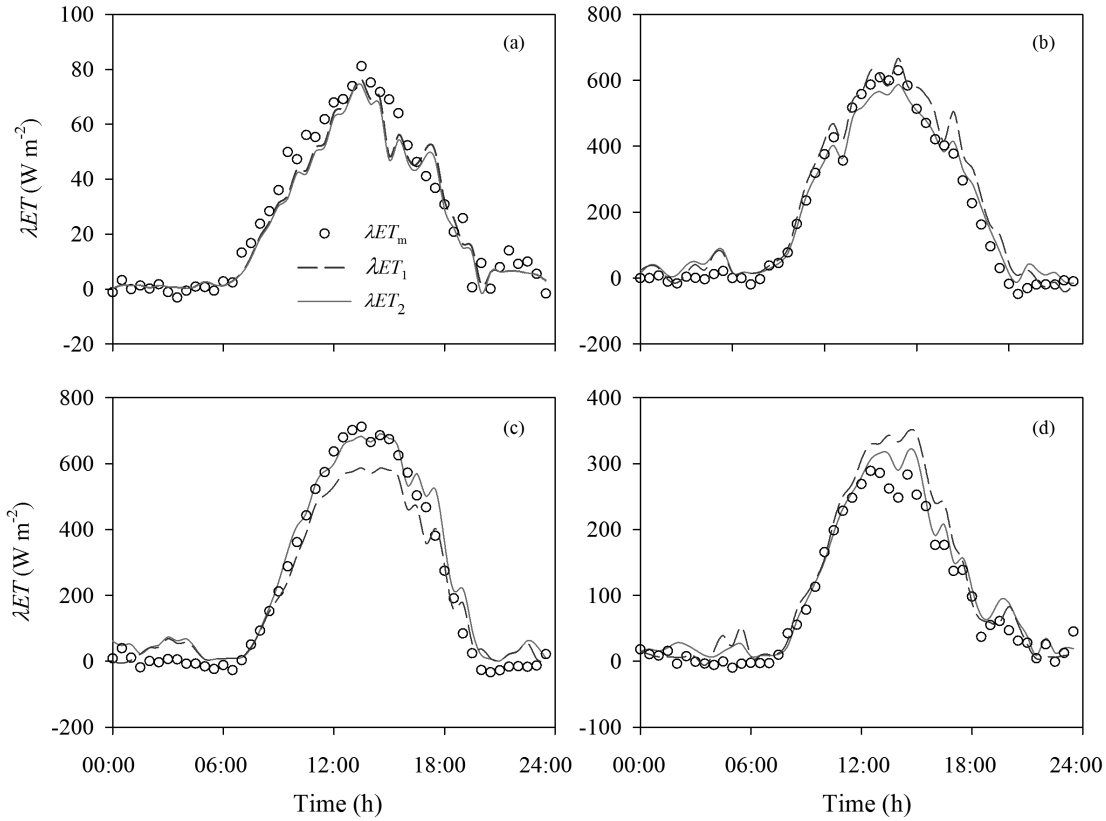

Figure 6. Diurnal variations of half-hourly crop evapotranspiration (λET) calculated by the dual-source with the big-leaf (λET_1) and dual-leaf models (λET_2), and measured λET (λET_m), respectively for four typical clear-sky days in different growth stages of maize in 2009. Leaf area index (*LAI*) was 0.16, 2.62, 5.38 and 2.99, on (a) May 22, (b) June 23, (c) July 27, and (d) September 17, respectively.
doi:10.1371/journal.pone.0095584.g006

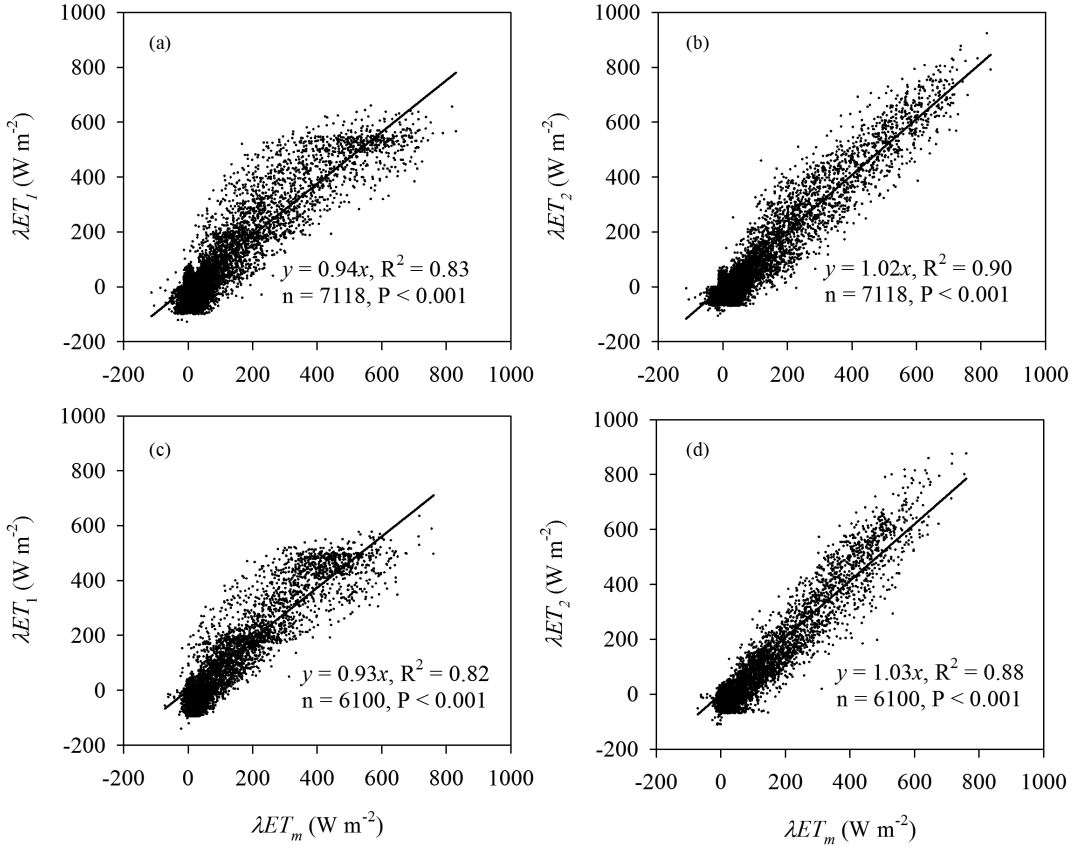

Figure 7. Comparison between half-hourly estimated evapotranspiration by the dual-source with the big-leaf (λET_1) and dual-leaf models (λET_2) versus measured λET by eddy covariance (λET_m) during the entire growth period of maize in (a and b) 2009 and (c and d) 2010.
doi:10.1371/journal.pone.0095584.g007

The extractable soil water in the root zone (θ_E) was significantly different between the two years. Before the first and second irrigation events in 2010, there were 9 and 12 days of θ_E below 50% total available water in the root zone (*TAW*), which was regarded as a threshold of crop water stress [13]. Conversely, most θ_E was higher than 50% of *TAW* in 2009. All of these differences led to differing λET and its components, which provided a good dataset to test the big-leaf and dual-leaf models over two different hydrometeorological and management strategies.

The scatterplots of half-hourly λET exhibited that λET_1 was overestimated for lower values and underestimated for higher values, respectively (Fig. 7a and 7c). Total λET_1 was underestimated, with a slope of linear regression of 0.94 ($R^2 = 0.83$) and 0.93 ($R^2 = 0.82$), respectively, for 2009 and 2010. RMSE was 72.22 and 70.97 W m^{-2}, and d was 0.9521 and 0.9472 for 2009 and 2010, respectively (Table 2). In contrast, there was good data-model agreement between measurements and estimated half-hourly λET_2 in 2009 and 2010 (Fig. 7b and 7d). The slopes of linear regressions between the estimates and measurements were 1.02 and 1.03, with R^2 of 0.90 and 0.88, RMSE of 58.06 and 62.31 W m^{-2} and d of 0.9706 and 0.9626 for 2009 and 2010, respectively (Table 2). Daily estimated λET_2 enhanced data-model agreement, with R^2 of 0.91 for the 2 years despite the linear slopes were the same as those of half-hourly values (data not shown). The statistical test showed that the slopes were not significantly different with one ($P = 0.114$ and 0.092), and the intercepts were not significantly different with zero ($P = 0.215$ and 0.174) for the 2 years.

Seasonal variations of daily estimated and measured E_s using Eq. (15) combined with Eqs. (39) and (40) are presented in Fig. 8 for 2009 and 2010. Both the dual-source big-leaf and dual-leaf models could capture the variability of E_s even when irrigation or precipitation occurred and when the canopy partially covered the ground during the initial growth stages. However, daily values of E_{s1} were underestimated at the early and late stages and overestimated at the middle stage (Fig. 8a and b). In general, total E_{s1} was underestimated by 5% and 7% for 2009 and 2010, respectively (Fig. 8c and d). In contrast, there was satisfactory data-model agreement between predicted and measured E_s using the DSDL model for the two years. The slopes of linear regressions between estimates and measurements were 1.02 ($R^2 = 0.68$) and 1.01 ($R^2 = 0.73$), with RMSE of 0.1220 and 0.1565 mm d^{-1} and d of 0.9129 and 0.9218 for 2009 and 2010, respectively (Table 2).

Discussion

In this paper, we have extended the big-leaf model by developing a dual-leaf model. The dual-leaf model presented here is an improvement over the previous big-leaf model, as more realistic non-uniform vertical profiles of radiation and stomatal conductance are now incorporated into the model. The penetration of beam radiation, its variation and the dynamics of sunlit and shaded *LAI* throughout the day all affect the ability of the big-leaf model to simulate diurnal changes in G_{sc} [18,29]. In the dual-leaf model, these canopy features can be explicitly incorporated by dividing the canopy into sunlit and shaded fractions and modeling

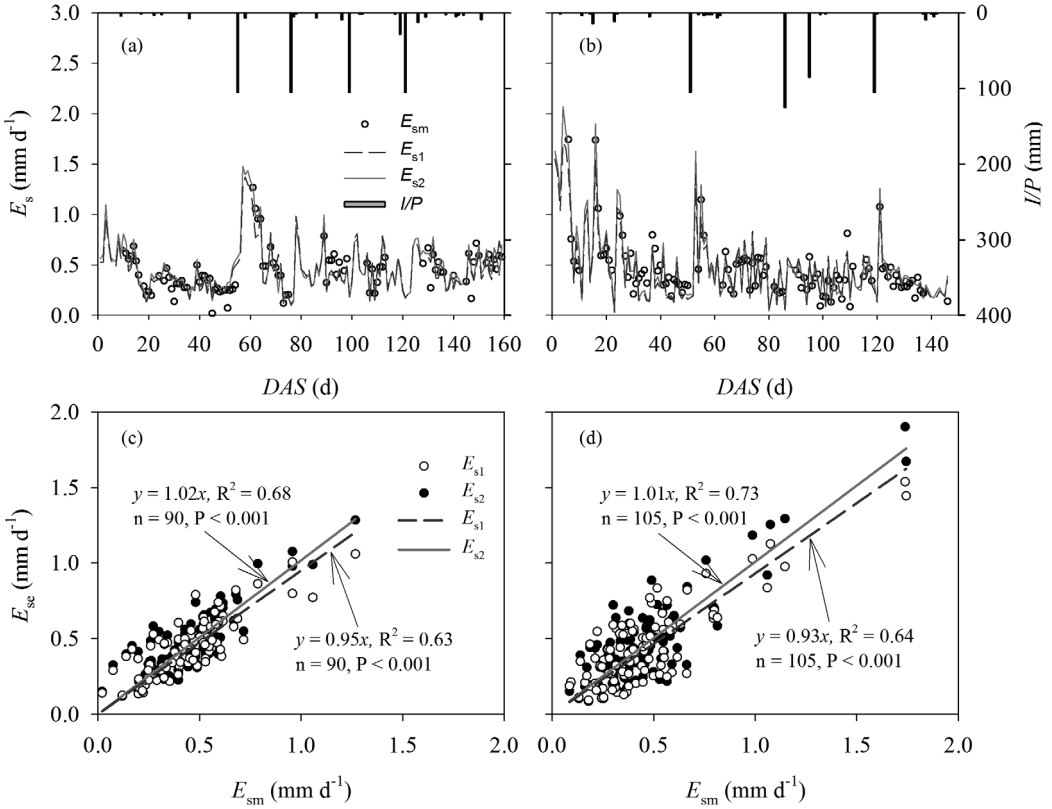

Figure 8. Comparison between daily estimated soil evaporation (E_{se}) by the dual-source with the big-leaf (E_{s1}) and dual-leaf models (E_{s2}) versus measurements (E_{sm}) during the entire growth period of maize in 2009 and 2010. Seasonal variations of the estimated and measured E_s against days after sowing (*DAS*) are presented in (a) and (b). The linear regressions between them are presented in (c) and (d).
doi:10.1371/journal.pone.0095584.g008

each fraction of G_{sc} by scaling up the respective stomatal conductance separately. It is more complex than the big-leaf model, but the dynamic partitioning of *LAI* and irradiance between sunlit and shaded leaves has further reduced the errors associated with simplifying the leaves to only a big-leaf using either the total or empirically effective *LAI*.

The ability of the dual-leaf model was examined by comparing the estimated values and actual measurements. In contrast to significant errors by the big-leaf model, the dual-leaf model accurately reproduced the variation of G_{sc} (Fig. 4 and 5). One reason the dual-leaf model works so well is that it accommodates the nonlinear response of stomata to light [25,40]. Stomata-light responses of leaves can vary with depth in the canopy and this variation can be incorporated by partitioning the canopy into several layers and estimating the sunlit and shaded leaf fractions in each layer [20,34]. However, usually this is not necessary and a single, representative light response curve can be used for the entire canopy [17,40]. In the dual-leaf model, the entire G_{sc} may be calculated by summing contributions of sunlit and shaded leaves. These two contributions are added separately because sunlit leaves will be light-saturated while shaded leaves will be in the linear portion of the light-stomata relationship [18,33]; thus G_{sc} is not proportional to average light levels [18]. Because of the nonlinear relationship between stomatal conductance and PAR, the predicted G_{sc} will be overestimated when the average absorbed PAR is used to scale up the leaf stomatal conductance for the entire canopy as in the big-leaf model [17,40]. On the other hand, the G_{sc} is underestimated when the effective *LAI* is used to scale up the leaf stomatal conductance at higher *LAI* ((Fig. 4c). Since the nonlinear relationship was considered and the sunlit-shaded method was introduced in the dual-leaf model, estimates using the dual-leaf model closely match the measured G_{sc} (Fig. 4 and 5).

The performance of the DSDL for estimating λET was investigated. The DSDL is robust for estimating λET over a range of canopy leaf areas and environmental variables (Fig. 6, Fig. 7 and Table 2). The good data-model agreement indicated the strengths of the DSDL model as a model framework and the reference for validating other approaches of calculating the G_{sc} using the dual-leaf model. Our framework of modeling λET also provided a soil evaporation estimation model Eq.(15) with a modified soil surface resistance term, which is useful for enhancing crop production by reducing the E_s fraction of λET [10,15].

The DSDL model is physically process-based, yet sufficiently simple to be effectively parameterized. The dual-leaf model requires only four additional equations, Eqs (32), (33), (43) and (44), beyond those required in the model of leaf stomatal conductance, to calculate the *LAI* and absorbed irradiance of the sunlit and shaded leaves. This simplicity makes it attractive for incorporation into in crop models, land surface schemes, and regional or global water cycle studies [29,40]. This model can also be used to assess effects of climate change on crop ecophysiology.

Conclusions

In this paper, a dual-leaf model for scaling-up stomatal conductance from the leaf to the canopy level was developed through the dynamic partitioning of the leaf area index and irradiance between sunlit and shaded leaves. In the model, canopy stomatal conductance was calculated by dividing the canopy into

sunlit and shaded fractions and each fraction was modeled separately based on the absorbed irradiances. The dual-leaf model provided estimates of G_{sc} which were nearly the same as measurements, and were significantly more accurate than those of the big-leaf model. Our results showed excellent agreements between λET measurements gathered by the eddy covariance technique over an irrigated maize field during 2009 and 2010 under two different hydrometeorological and management conditions, and estimates of λET using the DSDL. The framework of the model can also satisfactorily estimate soil evaporation. Our proposed model provides an alternative approach to calculate λET, which is simple and attractive for incorporation into other comprehensive crop models.

Supporting Information

Appendix S1 Resistances calculations and solar geometry. (DOCX)

Acknowledgments

We thank the two anonymous reviewers for their constructive comments that have helped to improve the manuscript.

Author Contributions

Conceived and designed the experiments: RD SK TD. Performed the experiments: RD YZ. Analyzed the data: RD YZ. Contributed reagents/materials/analysis tools: SK TD. Wrote the paper: RD SK TD XH YZ.

References

1. Leuning R, Zhang YQ, Rajaud A, Cleugh H, Tu K (2008) A simple surface conductance model to estimate regional evaporation using MODIS leaf area index and the Penman-Monteith equation. Water Resources Research 44: W10419, doi:10.1029/2007WR006562.
2. Pereira LS, Perrier A, Allen RG, Alves I (1999) Evapotranspiration: concepts and future trends. Journal of Irrigation and Drainage Engineering 125: 45–51.
3. Ding R, Kang S, Li F, Zhang Y, Tong L (2013) Evapotranspiration measurement and estimation using modified Priestley–Taylor model in an irrigated maize field with mulching. Agricultural and Forest Meteorology 168: 140–148.
4. Zhang X, Chen S, Sun H, Shao L, Wang Y (2011) Changes in evapotranspiration over irrigated winter wheat and maize in North China Plain over three decades. Agricultural Water Management 98: 1097–1104.
5. Katerji N, Rana G (2006) Modelling evapotranspiration of six irrigated crops under Mediterranean climate conditions. Agricultural and Forest Meteorology 138: 142–155.
6. Irmak S, Mutiibwa D (2010) On the dynamics of canopy resistance: Generalized linear estimation and relationships with primary micrometeorological variables. Water Resources Research 46: W8526, doi:10.1029/2009WR008484.
7. Pieruschka R, Huber G, Berry JA (2010) Control of transpiration by radiation. Proceedings of the National Academy of Sciences 107: 13372–13377.
8. Hu Z, Yu G, Zhou Y, Sun X, Li Y, et al. (2009) Partitioning of evapotranspiration and its controls in four grassland ecosystems: Application of a two-source model. Agricultural and Forest Meteorology 149: 1410–1420.
9. Er-Raki S, Chehbouni A, Boulet G, Williams DG (2010) Using the dual approach of FAO-56 for partitioning ET into soil and plant components for olive orchards in a semi-arid region. Agricultural Water Management 97: 1769–1778.
10. Ding R, Kang S, Zhang Y, Hao X, Tong L, et al. (2013) Partitioning evapotranspiration into soil evaporation and transpiration using a modified dual crop coefficient model in irrigated maize field with ground-mulching. Agricultural Water Management 127: 85–96.
11. Shuttleworth WJ (2007) Putting the "vap" into evaporation. Hydrology and Earth System Sciences 11: 210–244.
12. Monteith JL, Unsworth MH (2008) Principles of Environmental Physics. New York, USA: Academic Press. 418 p.
13. Allen RG, Pereira LS, Raes D, Smith M (1998) Crop Evapotranspiration: Guidelines for computing crop water requirements. Rome, Italy: FAO Irrigation and Drainage Paper, No. 56. 300 p.
14. Shuttleworth WJ, Wallace JS (1985) Evaporation from sparse crops-an energy combination theory. Quarterly Journal of the Royal Meteorological Society 111: 839–855.
15. Zhu G, Su Y, Li X, Zhang K, Li C (2013) Estimating actual evapotranspiration from an alpine grassland on Qinghai-Tibetan plateau using a two-source model and parameter uncertainty analysis by Bayesian approach. Journal of Hydrology 476: 42–51.
16. Zhang B, Kang S, Li F, Zhang L (2008) Comparison of three evapotranspiration models to Bowen ratio-energy balance method for a vineyard in an arid desert region of northwest China. Agricultural and Forest Meteorology 148: 1629–1640.
17. Campbell GS, Norman JM (1998) An Introduction to Environmental Biophysics. New York, USA: Springer-Verlag. 286 p.
18. Irmak S, Mutiibwa D, Irmak A, Arkebauer TJ, Weiss A, et al. (2008) On the scaling up leaf stomatal resistance to canopy resistance using photosynthetic photon flux density. Agricultural and Forest Meteorology 148: 1034–1044.
19. Ross J (1976) Radiative transfer in plant communities. In: Monteith JL, edito. Vegetation and the Atmosphere: Principles. New York, USA: Academic Press. 13–55.
20. Pyles RD, Weare BC, Pawu KT (2000) The UCD Advanced Canopy Atmosphere Soil Algorithm: Comparisons with observations from different climate and vegetation regimes. Quarterly Journal of the Royal Meteorological Society 126: 2951–2980.
21. Baldocchi D, Meyers T (1998) On using eco-physiological, micrometeorological and biogeochemical theory to evaluate carbon dioxide, water vapor and trace gas fluxes over vegetation: a perspective. Agricultural and Forest Meteorology 90: 1–25.
22. Raupach MR, Finnigan JJ (1988) 'Single-layer models of evaporation from plant canopies are incorrect but useful, whereas multilayer models are correct but useless': Discuss. Functional Plant Biology 15: 705–716.
23. Sinclair TR, Murphy CE, Knoerr KR (1976) Development and evaluation of simplified models for simulating canopy photosynthesis and transpiration. Journal of Applied Ecology: 813–829.
24. Zhang B, Liu Y, Xu D, Cai J, Li F (2011) Evapotranspiraton estimation based on scaling up from leaf stomatal conductance to canopy conductance. Agricultural and Forest Meteorology 151: 1086–1095.
25. Leuning R, Kelliher FM, De Pury DGG, Schulze ED (1995) Leaf nitrogen, photosynthesis, conductance and transpiration: scaling from leaves to canopies. Plant, Cell and Environment 18: 1183–1200.
26. Shuttleworth WJ, Gurney RJ (1990) The theoretical relationship between foliage temperature and canopy resistance in sparse crops. Quarterly Journal of the Royal Meteorological Society 116: 497–519.
27. Hou X, Wang F, Han J, Kang S, Feng S (2010) Duration of plastic mulch for potato growth under drip irrigation in an arid region of Northwest China. Agricultural and Forest Meteorology 150: 115–121.
28. Weiss A, Norman JM (1985) Partitioning solar radiation into direct and diffuse, visible and near-infrared components. Agricultural and Forest meteorology 34: 205–213.
29. De Pury D, Farquhar GD (1997) Simple scaling of photosynthesis from leaves to canopies without the errors of big-leaf models. Plant Cell and Environment 20: 537–557.
30. Jarvis PG (1976) The interpretation of the variations in leaf water potential and stomatal conductance found in canopies in the field. Philosophical Transactions of the Royal Society of London. Series B, Biological Sciences 273: 593–610.
31. Whitley R, Medlyn B, Zeppel M, Macinnis-Ng C, Eamus D (2009) Comparing the Penman-Monteith equation and a modified Jarvis-Stewart model with an artificial neural network to estimate stand-scale transpiration and canopy conductance. Journal of Hydrology 373: 256–266.
32. Stewart JB (1988) Modelling surface conductance of pine forest. Agricultural and Forest Meteorology 43: 19–35.
33. Farquhar GD, Sharkey TD (1982) Stomatal conductance and photosynthesis. Annual Review of Plant Physiology 33: 317–345.
34. Norman JM (1979) Modeling the complete crop canopy. In: Barfield G, edito. Modification of the Aerial Environment of Plants: American Society of Agricultural Engineers. 249–280.
35. Sun SF (1982) Moisture and heat transport in a soil layer forced by atmospheric conditions. Storrs: University of Connecticut.
36. Mauder M, Foken T (2004) Documentation and instruction manual of the eddy covariance software package TK2. Work Report University of Bayreuth, Dept. of Micrometeorology 26: 1614–8916.
37. Ding R, Kang S, Li F, Zhang Y, Tong L, et al. (2010) Evaluating eddy covariance method by large-scale weighing lysimeter in a maize field of northwest China. Agricultural Water Management 98: 87–95.
38. Willmott CJ (1982) Some comments on the evaluation of model performance. Bulletin of the American Meteorological Society 63: 1309–1313.
39. Ding R, Tong L, Li F, Zhang Y, Hao X, et al. (2014) Variations of crop coefficient and its influencing factors in an arid advective cropland of northwest China. Hydrological Processes, DOI:10.1002/hyp.10146.
40. Wang YP, Leuning R (1998) A two-leaf model for canopy conductance, photosynthesis and partitioning of available energy I: Model description and comparison with a multi-layered model. Agricultural and Forest Meteorology 91: 89–111.
41. Brutsaert W (1982) Evaporation into the Atmosphere: Theory, History, and Applications. Dordrecht, Netherlands: Kluwer Academic Publishers. 299 p.
42. Meyers TP, Paw U (1987) Modelling the plant canopy micrometeorology with higher-order closure principles. Agricultural and Forest Meteorology 41: 143–163.